



1 **Worldwide soil moisture changes driven by future hydro-** 2 **climatic change scenarios**

3 Lucile Verrot¹, Georgia Destouni¹

4 ¹Department of Physical Geography & Bolin Centre for Climate Research, Stockholm University, SE-106 91
5 Stockholm, Sweden

6 *Correspondence to:* Lucile Verrot (lucile.verrot@natgeo.su.se)

7

8 **Abstract.** Soil moisture is a key variable in hydrology, ecology, and climate change science. It is also of
9 primary importance for the agricultural and water resource sectors of society. This paper investigates how hydro-
10 climatic changes, projected by 14 CMIP5 models and for different radiative forcing (RCP) scenarios to occur from
11 2006-2025 to 2080-2099, may affect different soil moisture aspects in 81 large catchments worldwide. Overall, for
12 investigated changes in dry/wet event occurrence and in average value and inter-annual variability of seasonal
13 water content, different RCP scenarios imply opposite directions of change in around half or more of the study
14 catchments. Regardless of RCP scenario, the greatest projected changes are found for the inter-annual variability of
15 seasonal soil water content. Especially for the dry-season water content, large increases in inter-annual variability
16 emerge for several large catchments over the world; the considered RCP scenario determines precisely which these
17 catchments are.

18 **1. Introduction**

19 Soil moisture plays a major role in the hydrologic and climatic systems, by influencing the water and
20 energy partitioning between the atmosphere and the subsurface (Corradini, 2014; Seneviratne et al., 2010). It also
21 affects and is affected by the water fluxes into and from the groundwater system (Destouni and Verrot, 2014), and
22 is of major importance for human societies (Oki and Kanae, 2006). Soil moisture is a dynamic variable defined as
23 the volume of water in a given volume of soil. It is also spatially heterogeneous, and depends on both dynamic
24 (e.g. vegetation, spatial distribution of hydro-climatic conditions) and static factors (soil type, topography)
25 (Destouni and Cvetkovic, 1989; Russo, 1998; Mohanty et al., 2000)



26 Long-term and large-scale shifts in climate as well as in land-use and water-use conditions in the
27 landscape (Destouni et al., 2013; Jaramillo and Destouni, 2014) are shown to impact the hydro-climate and the
28 water resources in various regions of the world. Considerable hydro-climatic shifts have occurred in the past
29 (Jaramillo and Destouni, 2015) and are expected to occur in the future (Bring et al., 2015) locally and globally. In
30 particular for future projections, the hydro-climatic shifts are uncertain and depend on the path that our societies
31 will take regarding greenhouse gas (GHG) emissions (Peters et al., 2013; IPCC, 2014) and on the societal paths for
32 local land- and water-uses (Destouni et al., 2010; Jarsjö et al., 2012).

33 Hydro-climatic changes impact soil moisture conditions at different temporal and spatial scales (D'Odorico et al.,
34 2000; Destouni and Verrot, 2014; Destouni and Verrot, 2015). Such impacts may, for instance, be derived from
35 complex modeling of soil water hydraulics or directly from large-scale climate model outputs (Wu et al., 2015;
36 Dirmeyer et al., 2013; Kumar et al., 2014). While the former approach does not readily allow for the complex
37 calculations to be carried out for long time periods and on regional to global scales, the latter approach is limited in
38 its process representation and soil depth coverage. Attempting to bridge such quantification gaps, Destouni and
39 Verrot (2014) and Verrot and Destouni (2015) have developed a modelling framework that links large-scale hydro-
40 climatic flux variables with soil hydraulic properties over whole catchments and distinguishes the dynamic
41 interactions between the unsaturated zone and the groundwater zone down to any soil depth of interest.

42 The modeling framework of Destouni and Verrot (2014) and Verrot and Destouni (2015) has been applied
43 to various parts of the world and its results have been tested against independent observation data. The latter
44 include data from the GRACE satellites (CSR-RL05, from Swenson (2012), Landerer and Swenson (2012),
45 Swenson and Wahr (2006)) regarding large-scale water storage changes and data from local measurements of soil
46 water content and groundwater level (Verrot and Destouni (2016)). This data-model testing has provided support
47 for the model realism in reproducing long-term time series of soil moisture across various catchment scales and
48 world regions along steep climate gradients. The present study will use this modeling framework to quantify
49 possible future changes of soil moisture conditions in a worldwide set of large catchments, as implied by the phase
50 5 of the Coupled Model Intercomparison Project (CMIP5) (Taylor et al., 2012).

51 Using this framework, we investigate projected climate-driven change in soil water content over the
52 unsaturated zone, specifically regarding changes in the occurrence frequency of particularly dry and wet events in
53 81 large hydrological catchments spread over the world (Fig. 1). Furthermore, we investigate the long-term



54 average conditions and the inter-annual variability around these for the soil water content in the dry and the wet
55 season of these catchments.

56

57 To investigate the projected climate-driven changes in the addressed soil moisture measures for the 81
58 study catchments, we use relevant hydro-climatic outputs from the CMIP5 model ensemble for the time period
59 2006-2099 and compare resulting soil water content conditions between the recent-to-near-future 20-year period
60 2006-2025 and the far-future 20-year period 2080-2099. These comparisons are further made for two different
61 Representative Concentration Pathways (RCP) scenarios: RCP 2.6 (van Vuuren et al., 2007) and RCP 8.5 (Riahi et
62 al., 2011).

63 2. Material and methods

64 2.1 Modeling approach

65 From the modeling framework proposed by Destouni and Verrot (2014), we focus here on the time-
66 variable depth-averaged soil water content over the unsaturated zone θ_{uz} [-], which is in that framework evaluated
67 as:

$$\theta_{uz} = \left(\frac{q}{K_s}\right)^\beta (\theta_s - \theta_{ir}) + \theta_{ir} \approx \left(\frac{R_{eff}}{K_s}\right)^\beta (\theta_s - \theta_{ir}) + \theta_{ir} \quad (1)$$

68

69 In Eq. (1), q [LT^{-1}] is average vertical soil water flux through the unsaturated zone, R_{eff} [LT^{-1}] is a catchment-scale
70 approximation of q in terms of effective subsurface runoff through a whole catchment (explained further below),
71 K_s [LT^{-1}] is saturated hydraulic conductivity, θ_{ir} [-] is residual irreducible soil water content, $\beta = \alpha/(3\alpha + 2)$ [-] and
72 α [-] is a characteristic soil texture parameter linked to the pore size distribution of different soil types (Rawls et
73 al., 1982; Saxton et al., 1986). Furthermore, θ_s is saturated soil water content, which can be equated to porosity
74 (Kumar, 1999; Entekhabi et al., 2010). The θ_{uz} quantification in Eq. (1) is based on the Brooks and Corey (1964)
75 model of unsaturated hydraulic conductivity K [LT^{-1}]:

$$K(\theta_{uz}) = K_s \left(\frac{\theta_{uz} - \theta_{ir}}{\theta_s - \theta_{ir}}\right)^{1/\beta} \quad (2)$$

76 Alternative expressions of K as function of θ_{uz} are also available from van Genuchten (1980) and Morel-Seytoux et
77 al. (1996) with soil parameters that are related to those of Brooks and Corey.



78 The first part of Eq. (1) is based on a first-order approximation and extension from the Brooks and Corey
79 Eq. (2), considering unit hydraulic gradient and gravity as a dominant, even though not the only, driver of large-
80 scale flow through the unsaturated zone. This approximation was introduced and used by Dagan and Bresler
81 (1979) and Bresler and Dagan (1981), and in multiple studies thereafter (e.g., Destouni and Cvetkovic, 1989, 1991;
82 Destouni, 1993; Destouni and Graham, 1995). The approximation implies that, the unsaturated hydraulic
83 conductivity K in Eq. (2) can be equated to the average vertical soil water flux through the unsaturated zone q , with
84 further equation rearrangement leading to the first part of Eq. (1). The studies of Destouni and Verrot (2014),
85 Verrot and Destouni (2015, 2016) further introduced the second part of Eq. (1) for data-based quantification of the
86 temporal variability of the large-scale depth-average unsaturated water content θ_{uz} around its long-term average
87 value. This equation part expresses the main assumption that, on the scale of a whole catchment, both the long-
88 term average value of q and the temporal q variability around it can be estimated from and constrained by available
89 observation data for runoff R through the catchment.

90 Specifically, the assumption is that q can be approximated by an effective subsurface runoff component
91 $R_{eff} = \gamma R$ [LT^{-1}] (with $0 \leq \gamma \leq 1$) that feeds water through the subsurface into the total runoff R [LT^{-1}] of the catchment
92 over some considered time period. This subsurface runoff component R_{eff} complements the runoff component $(1-$
93 $\gamma)R$ of overland and pure (not fed by subsurface water into the) surface water flow, which also adds to the total R
94 over the same time period. Published simulations have quantified and shown $\gamma = R_{eff}/R$ to be typically above 0.5 and
95 in many cases close to 1 for a wide range of investigated temperate, through cold, to permafrost region conditions
96 (Bosson et al., 2012). In the present study, γ values and their variability in time do not need to be explicitly
97 evaluated, because CMIP5 model output includes directly quantified R_{eff} times series for future climate change
98 scenarios, as explained in the subsequent section 2.2.

99 For a long climatic time period of twenty or more years, the long-term average R_{eff} should relatively well
100 approximate the long-term average q because the subsurface water storage change can be expected to be close to
101 zero when averaged over such long time periods (Jaramillo et al., 2013; Destouni et al., 2013; Jaramillo and
102 Destouni, 2015). Over shorter time scales, such as a month or a day, however, q and R_{eff} may differ due to non-zero
103 water storage change occurring over the same time, with q through the soil being transiently partitioned between
104 feeding water into R_{eff} and increasing water storage in the soil, and conversely R_{eff} being fed by both q and a
105 transient decrease in soil water storage. However, even under such conditions of non-zero water storage change,
106 the relative variability of R_{eff} around its long-term average value may still be relevant and sufficient for estimating



107 the corresponding relative variability of large-scale depth-average unsaturated water content θ_{uz} around its long-
 108 term average value, through the second part of Eq. (1). This assumption is tested by direct comparison of θ_{uz} results,
 109 as given by the second part of Eq. (1), against independent observation data provided from GRACE (Swenson,
 110 2012; Landerer and Swenson, 2012; Swenson and Wahr, 2006) supports the main model assumption (Verrot and
 111 Destouni, 2016). The comparison support (i.e., does not falsify) the assumption by showing that the model results
 112 realistically capture the temporal variability in large-scale water storage change around its expected near-zero long-
 113 term average value, across various large catchments around the world (Fig. 2).

114

115 Furthermore, previous work by Jaramillo and Destouni (2013) has explicitly investigated the effects of
 116 accounting or not accounting for observed water storage changes on the variability of main water fluxes in a
 117 catchment-scale water balance. Specifically they quantified for different catchments the effect of estimating
 118 catchment-scale evapotranspiration ET [LT^{-1}] as simply $ET=P-R$ or as $ET=P-R-\Delta S$, where P , R and ΔS are
 119 observed precipitation, runoff and storage change, respectively (all with dimensions [LT^{-1}]). Their results show
 120 somewhat greater short-term fluctuations around essentially the same longer-term ET variation if the observed non-
 121 zero ΔS is accounted for compared to if it is not. Similar effects, of relatively minor underestimation of relatively
 122 short-term fluctuations of θ_{uz} around its essentially captured seasonal and longer-term variation, are also expected
 123 here from neglecting the influence of ΔS -driven differences between q and R_{eff} in the estimation of θ_{uz} by Eq. (1).
 124 To even further quantify and clarify this influence for the present study, consider for example the cumulative water
 125 storage change ΔS as:

$$\Delta S = \left(\sum_{i=1}^n P_i - ET_i - R_i \right) / n \quad (3)$$

126 with P , ET , R and ΔS all being monthly water fluxes and n being the total number of months with associated
 127 CMIP5 flux outputs ($n=1128$). The resulting cumulative ΔS over the whole study period accounts then for less than
 128 1% of the mean monthly P , on average across all 81 study catchments (the average value across catchments is
 129 0.75% and the standard deviation is 2.3%). This quantification provides further support for the assumption of
 130 insignificant long-term change in subsurface water storage that underlies the approximation of $q \approx R_{eff}$ in Eq. (1)

131

132 **2.2 Use of CMIP5 model output data**



133 The aim of the present work is to study climate-driven change patterns and statistics of θ_{ice} , as quantified
 134 by the second part of Eq. (1), in the present 81 study catchments, spread over the world. The study uses relevant
 135 hydro-climatic outputs for estimating R_{eff} from two of the CMIP5 scenarios for the 21st century, the RCP 2.6 and
 136 RCP 8.5 scenarios. Those scenarios represent a low (RCP 2.6) and a high (RCP 8.5) GHG-increase scenario,
 137 corresponding to reaching a radiative forcing of 2.6 W.m⁻² and 8.5 W.m⁻² by the end of the 21st century,
 138 respectively. The relevant CMIP5 model outputs were downloaded from the World Data Center for Climate
 139 (WDCC) available from the Deutsche Klimarechenzentrum GmbH website (<http://cera-www.dkrz.de/WDCC>).

140 The CMIP5 models' outputs of relevance for estimating R_{eff} are the mean monthly surface runoff
 141 (overland flow, denoted $mrros$) and the total runoff (denoted $mrro$) in the CMIP5 output files. The total runoff
 142 $mrro$ is the sum of the overland flow and the soil-groundwater flow (in short underground flow), both of which
 143 eventually feed into the streams of each catchment. With $mrros$ then being just the overland flow, R_{eff} could be
 144 calculated directly from these CMIP5 model outputs (without need for separate evaluation of the factor $\gamma=R_{eff}/R$)
 145 as:

146

$$R_{eff} = mrro - mrros \quad (4)$$

147

148 For evaluation of Eq. (4), the model output values for $mrro$ and $mrros$, given from the CMIP5 modeling
 149 in units kg.m⁻².s⁻¹, were transformed to relevant units for R_{eff} [LT⁻¹] using the water density value of 1000 kg.m⁻³.
 150 Furthermore, in errata files published for the CMIP5 models GISS-E2-H and GISS-E2-R (with the errata files
 151 available online only, at: <http://data.giss.nasa.gov/modelE/ar5/>), it is specified that for those two models the
 152 variable $mrro$ is the underground flux only, in contrast to the definition of $mrro$ in all other models (underground
 153 flux + surface runoff). For those two models, R_{eff} is therefore directly equated to $mrro$.

154 In addition to the two R_{eff} -related variables, we also used from the CMIP5 model outputs the precipitation
 155 variable pr (kg.m⁻².s⁻¹). This was used to determine the model-implied dry and wet season for each selected study
 156 catchment, which was also compared with a corresponding dry and wet season determination based on observation
 157 data for precipitation, as described further in section 2.4.

158

159 2.3 Selection of study catchments and CMIP5 models



160 The 81 study catchments were chosen in analogy with such selection basis in previous work (Bring et al.,
161 2015), taking into account that the catchments should be large enough for sufficient coverage by the commonly
162 coarse spatial resolution of global climate models. In the selection process, we first extracted relevant model output
163 values for 608 catchments in the Global Runoff Data Center (GRDC, 2015) with an area equal or greater than
164 100'000 km². The model output values were then averaged to represent monthly conditions over each catchment.

165 For the catchment-scale use of model output, we further also identified 20 CMIP5 models that could
166 provide all three variables of interest (*mrro*, *mrros* and *pr*) for download over the whole study period (2006-2099).
167 However, for some catchments and for some models, the time series provided for *mrro* and/or *mrros* included just
168 a constant number over time. Models and catchments with too many such constant time series were discarded (see
169 SM section S1 for more details on this selection criterion).

170 A second selection basis for the study models and catchments was to discard the model-catchment
171 combinations that yielded negative catchment-scale R_{eff} values. Knowing that a positive flux value in CMIP5
172 output implies a flux leaving the considered atmospheric grid cell, a negative flux value thus quantifies a flux of
173 water that must enter the atmospheric cell from the soil. The implication of negative catchment-scale monthly R_{eff}
174 is then that an upward flux of water from the soil to the atmosphere (independent from and in addition to the
175 separately evaluated evapotranspiration flux in the same direction) is sustained on average over a whole catchment
176 and a whole month. Such a flow situation may be neither realistic nor consistent with the separately evaluated
177 evapotranspiration flux output from the same climate model, and is at least unusual compared to the more
178 generally expected flow situation of an excess amount of water being on average generated from precipitation
179 minus evapotranspiration on land and flowing as runoff toward the outlets of hydrological catchments. At any rate,
180 modeling soil water content conditions and statistics for such a negative R_{eff} flow situation is outside the scope of
181 the present soil moisture model and in contradiction with its basic flow approximations.

182 The two above-described catchment-model selection steps were repeated for each of the two considered
183 RCP 2.6 and RCP 8.5 scenarios and finally also all small remaining catchments that were nested into larger ones
184 were removed. This selection process yielded the final set of 81 study catchments (Fig. 1) and 14 CMIP5 models
185 (listed in SM Table S1) used in the present study (SM Table S2 lists the models and number of catchments
186 discarded in each selection step). The study catchments are spread around the globe, and clustered here for
187 discussion convenience into 6 regions, as shown on Fig. 1, in analogy with regional divisions made by the World
188 Meteorological Organization (WMO, 2014).



189

190 **2.4 Use of soil and precipitation data for the study catchments**

191 In addition to the runoff output data from the CMIP5 models, the calculation of unsaturated water content
192 θ_{uz} also requires catchment-characteristic values for the soil hydraulic properties included in Eq. (4). The dominant
193 USDA soil texture (Baldwin et al., 1928) for each catchment was extracted from the Harmonized World Soil
194 Database map (Nachtergaele et al., 2008; FAO, 2012). SM Fig. S1 shows the major soil textures within each
195 catchment and Table S3 lists soil parameter values for different soil textures from Rawls et al. (1982). The
196 parameter values from Table S3 that apply to the dominant soil texture within each catchment (Fig. S1) were used
197 to evaluate θ_{uz} for that catchment from Eq. (4).

198 Furthermore, we used the precipitation output pr from the CMIP5 models to determine the model-implied
199 dry and wet season extents for each selected study catchment and considered climatic time period. The used
200 definition of the dry season is the months during which 8% or less of the total annual precipitation falls (after
201 Koutsouris et al., (2015): the exact value is set to maximize the agreement between the CMIP5 precipitation time
202 series and that from the Global Precipitation Climatology Centre, GPCC), with the wet season then defined as the
203 remaining months of the year. Results for this season determination were obtained for each of the 81 study
204 catchments (Fig. 1) and for both the RCP 2.6 and the RCP 8.5 scenario from the ensemble mean precipitation
205 output of the 14 CMIP5 models (SM Table S1). These model-based results were further tested against a
206 corresponding data-implied dry-wet season determination obtained from the $1.0^\circ \times 1.0^\circ$ monthly precipitation
207 dataset provided by the Global Precipitation Climatology Center (GPCC, see Schneider et al., 2011). This model-
208 data comparison was made over the 9-year period (2006-2014) that is common between the GPCC dataset
209 (extending over 1901/01 – 2014/12) and the studied CMIP5 output period (2006-2099).

210 The comparison between the model- and data-based results for wet and dry season extent shows that the
211 results are largely consistent (SM Fig. S2). For both the RCP 2.6 and the RCP 8.5 scenario, 40% of the catchments
212 display perfect agreement on the dry season months, and for more than 85% of the catchments at least half of the
213 dry season months match between the data and the model results. From these comparative results, we concluded
214 that it is reasonable to study dry and wet season changes in soil moisture between the climatic periods 2006-2025
215 and 2080-2099 based on the season determination implied by the CMIP5 ensemble mean.

216



217 2.5 Ensemble-mean model study of soil moisture variability and change

218 The use of a model ensemble mean instead of a model-by-model study of climate change is widely found
219 in the literature as it has been shown to perform as well as good individual models (Sillman et al. 2013), and not
220 least so for hydro-climatic changes in the landscape (Jarsjö et al., 2012; Törnqvist et al., 2014; Asokan et al.,
221 2016). To use a model ensemble mean approach also in this soil moisture study of changes, it was useful to first
222 assess resulting differences among the used CMIP5 models (Table S1) in the temporal variability patterns of soil
223 moisture.

224 Figure S3 in SM illustrates the relative temporal variability (coefficient of variation CV, determined as the
225 inter-annual standard deviation divided by the long-term average value) of monthly average soil water content θ_{iz} ,
226 as obtained from each CMIP5 model (Table S1) over the entire time period of study (2006-2099). The individual
227 model results for each month of the year and each catchment show relatively small CV values (mostly below 0.25),
228 which also do not differ much among the 14 CMIP5 models. Some exceptions are notable: the model IPSL-
229 CM5A-MR displays a particularly high temporal variability in many catchments, and the two MPI models (MPI-
230 ESM-LR and MPI-ESM-MR) display a higher temporal variability than other models for some catchments.
231 However, for the other 11 models, the CV values for all months, both scenarios, and most catchments are
232 commonly less than 0.25.

233 This comparison of individual model results supports a further use of the model ensemble mean in the
234 following of this study by showing that inter-model differences are relatively small and obtained ensemble mean
235 results are thereby representative for most models regarding relative temporal soil moisture variability and change
236 around each model's long-term average soil moisture result. While the latter, absolute level of long-term average
237 soil moisture may vary greatly among models and thus exhibit large model uncertainty, the present study does not
238 focus on that model uncertainty but rather on determining what models tend to agree on, so that projected changes
239 of those soil moisture aspects of model agreement may be viewed as change projections with relatively low model
240 uncertainty. Hereafter, unless stated otherwise, the discussed and presented results are from the model ensemble
241 mean calculations.

242 For each of the two climatic periods 2006-2025 and 2080-2099 we have then derived the intra-annual
243 variability in monthly average water content θ_{iz} over the average annual cycle in each time period. Furthermore, we
244 have assessed the change from 2006-2025 to 2080-2099 in the occurrence frequency of wet and dry events; these
245 are defined as monthly average θ_{iz} values that exceed the 95% upper percentile θ_{iz} value (for wet events) or are



246 below the 5% percentile θ_{uz} value (for dry events) of the first period 2006-2025. Changes in wet and dry season
247 conditions of θ_{uz} have further been quantified in terms of the average value and the inter-annual variability around
248 it for seasonal θ_{uz} in 2006-2025 and in 2080-2099. The agreement of results obtained for any investigated variable
249 in the two scenarios RCP 2.6 and RCP 8.5 has also been calculated in terms of a simple agreement indicator as
250 detailed in SM section S3.

251 3. Results

252 Figure 3 shows results for the intra-annual variability in monthly average water content θ_{uz} in the two
253 climatic periods 2006-2025 and 2080-2099 for 6 study catchment examples, one in each WMO region; SM Fig. S4
254 shows corresponding results for all study catchments. These figures also show in more detail than in the SM Fig.
255 S3 the resulting inter-model variability (standard deviation) around the ensemble mean model result. Overall,
256 projected changes in intra-annual variability of monthly average θ_{uz} are relatively small, and mostly smaller than
257 the inter-model standard deviation around the ensemble mean result, representing a measure of model uncertainty,
258 for each climatic period.

259

260 The greatest relative changes in the occurrence frequency of both dry and wet θ_{uz} events, as
261 defined in section 2.5, are projected to occur under the scenario RCP 8.5 (Fig. 3). For this scenario, the catchment
262 Nam9 in southern US exhibits the greatest increase, by up to 80%, in the dry-event frequency in 2080-2099
263 relative to that in 2006-2025; this means that this catchment may reach a 9% frequency in 2080-2099 for the dry
264 events with only 5% frequency in 2006-2025. Under scenario RCP 2.6, the same catchment Nam9 is instead
265 projected to experience an increase in dry-event frequency by only up to 20%, i.e., reach a 6% frequency in 2080-
266 2099 for the dry events with 5% frequency in 2006-2025.

267

268 Overall, there are multiple catchments with projected opposite change directions in their dry-event
269 frequency under the two scenarios, including both decreases and increases under the RCP 2.6 scenario (Fig. 4a)
270 that shift to opposite increases and decreases, respectively, under the RCP 8.5 scenario (Fig. 4b). A whole
271 geographic pattern of dry-event frequencies mostly decreasing slightly in higher latitude regions (North America,
272 Europe, Northern Asia) and increasing slightly in lower latitude regions (South America, Africa, South East Asia,
273 Australia) under the RCP 2.6 scenario is shifted to a more heterogeneous pattern of spatial changes under the RCP



274 8.5 scenario. An analogous geographic pattern shift is also evident for the wet-event frequency; in this case a
275 geographic pattern of wet-event frequencies mostly increasing slightly in higher latitude regions and decreasing
276 slightly in lower latitude regions under the RCP 2.6 scenario (Fig. 4c) shifts to a more heterogeneous change
277 pattern, including also relatively large changes, under the RCP 8.5 scenario (Fig. 4d).

278 The greatest increase in wet-event frequency, by up to 50%, is projected for the southern
279 Brazil/Uruguay catchment Sam3, where a frequency of up to 7.5% may thus be reached for the wet events under
280 the scenario RCP 8.5. In contrast, under the RCP 2.6 scenario, a slight increase in wet-event frequency may instead
281 occur in this catchment. In general, the results in Fig. 4 show that the representative GHG concentration pathway
282 to the future, as represented by each RCP scenario, plays a key role for projected changes in the future occurrence
283 frequency of dry and wet soil moisture events around the world.

284 Shifts in geographic change patterns between the two RCP scenarios are also seen for relative
285 change in average soil water content during the dry and the wet season (Fig. 5). For both seasons, the average
286 water content θ_{wz} mostly increases slightly in the higher latitude regions and decreases slightly in the lower latitude
287 regions under the RCP 2.6 scenario (Fig. 5a and 5c). This pattern is again shifted to a more heterogeneous change
288 pattern, including also relatively large changes, under the RCP 8.5 scenario (Fig. 5b and 5d). Overall the projected
289 changes in seasonal average θ_{wz} are relatively small, up to a 15% increase for the dry season in several Arctic
290 region catchments and up to a 15% decrease in a few scattered catchments in North America, Europe and Africa
291 for the dry and/or the wet season.

292

293 The overall greatest projected relative changes are found for the inter-annual variability of seasonal θ_{wz}
294 (Fig. 6). Many catchment exhibit a +/- 40% increase/decrease in this inter-annual variability, for both seasons and
295 under both RCP scenarios. The greatest change is an up to 180% increase in inter-annual θ_{wz} variability for the dry
296 season in catchment Eur10 under the RCP 2.6 scenario. Several European, South East Asian and African
297 catchments also exhibit an up to 120% change in inter-annual variability of θ_{wz} during the dry season under the
298 RCP 8.5 scenario. The relatively large changes in inter-annual soil moisture variability, in particular during the dry
299 season, indicate increased drought risk for several catchments, with the geographic change pattern being in this
300 case heterogeneous and including scattered large-change catchments for both RCP scenarios.

301



302 The directions of change are opposite in many catchments between the two RCP 2.6 and RCP 8.5
303 scenarios for the event and the seasonal changes investigated in this study: in the frequency of dry and wet θ_{ic}
304 events (SM Fig. S5), in the average seasonal θ_{ic} (SM Fig. S6) and in the inter-annual variability of seasonal θ_{ic}
305 (SM Fig. S7). Overall, the latter changes in inter-annual variability of seasonal θ_{ic} exhibit the largest differences in
306 change direction between the two RCP scenarios. These opposite change directions are exhibited for a majority of
307 the catchments during the dry season (43 catchments), and for nearly as many catchments (40) during the wet
308 season.

309 4. Discussion

310 For most of the study catchments, the pattern of changes in frequency of wet/dry events (Fig. 3) is
311 consistent with that in average seasonal soil moisture (Fig. 5); the resulting Pearson correlation coefficient is -0.68
312 for RCP 8.5 and -0.75 for RCP 2.6 regarding the frequency of dry events and average soil moisture during the dry
313 season, and -0.68 for RCP 8.5 and -0.74 for RCP 2.6 regarding the frequency of wet events and average soil
314 moisture during the wet season. The consistency lies in that a catchment with increased average seasonal soil
315 moisture (occurs mostly in the higher latitude regions for both the dry and the wet season, Fig. 5) is likely to also
316 experience more frequent wet events or less frequent dry events (Fig. 4). However, there are individual catchment
317 exceptions to this common change pattern, for example in catchments Afr3 and Eur3, where the RCP 8.5 scenario
318 implies an increase in the frequency of wet events (Fig. 4d), while also implying a decrease in average seasonal
319 soil moisture during the wet season (Fig. 5d). Such a change situation may, for example, be explained by highly
320 increased short-term fluctuation magnitudes and thereby occurrence frequency for rare wet events during the wet
321 season even though the average seasonal soil moisture has decreased. Further study of specific wet and dry
322 fluctuation magnitudes and event frequency for each season instead of over the whole year as investigated here,
323 can shed light on such more unusual change situations.

324 The scenario RCP 8.5 yields generally higher change values for all types of changes and for both dry and
325 wet soil moisture events and seasons. This change pattern is most evident in the dry season results: in about 86% of
326 the catchments, the RCP 8.5 scenario yields higher absolute change in both the average seasonal soil moisture and
327 in its inter-annual variability during the dry season, while for the wet season the corresponding ratio is closer to
328 around 50% of the catchments being more strongly affected under RCP 8.5 than under RCP 2.6. Similarly, changes
329 in the frequency of wet and dry events are greater in 70% and 77% of the catchments, respectively, under RCP 8.5



330 than under RCP 2.6. Along with the finding that the two RCP scenarios yield different directions of change in 50%
331 of the catchments for dry conditions, and in 40% of the catchments for wet conditions, these findings show that the
332 representative GHG concentration pathway of forthcoming climate change is crucial for the directions and the
333 magnitudes of future soil moisture changes over the world.

334 The present 81 study catchments represent 27% of the Earth's land surface, which is a relatively
335 high sampling coverage for statistical analysis, like the present one, of the world soil moisture changes. The
336 commonly coarse resolution of global climate models does not allow for much more detailed, sub-regional, spatial
337 analysis than the present one, but more fine-resolved regional climate model outputs could be used for addressing
338 finer spatial detail and catchment resolution in follow-up work.

339 Although hydro-climatic changes greatly influence soil moisture changes, they are not the only predictors
340 of the latter. By them selves, precipitation, evapotranspiration, and R_{eff} -related (Eq. 4) outputs taken directly from
341 climate models correlate relatively poorly with the soil water content θ_{sz} (Eq. 3), with Pearson correlation
342 coefficients of 0.39, 0.28, and 0.45, respectively. The relatively poor direct correlation of these climate model
343 outputs to θ_{sz} is due mainly to the soil hydraulic parameter relation of θ_{sz} in Eq. (4), which non-linearly modulates
344 the θ_{sz} response to the hydro-climatic forcing. This non-linearity emphasizes the importance of assessing soil
345 moisture changes in relevant relation to soil constitutive equations rather than just directly from hydro-climatic
346 outputs of climate models.

347 In follow-up studies, agriculturally important growing seasons for different parts of the world can be
348 considered and accounted for similarly to the present analysis of wet and dry seasons. The growing season may in
349 some cases even correspond to the present wet season definition, for example for some tropical catchments, while
350 the present dry season definition may be more relevant for the growing season in Europe. Also groundwater level
351 variability and change should be investigated in future studies, for instance by extending the present analysis
352 approach to the full modeling framework of Destouni and Verrot (2014) and Verrot and Destouni (2015), in order
353 to investigate soil moisture effects of a changing groundwater table (and associated variable depth of the
354 unsaturated zone) within various soil depths of interest.

355 5. Conclusion

356 We have investigated how hydro-climatic changes, projected by 14 CMIP5 models to occur from 2006-
357 2025 to 2080-2099 under the two radiative forcing scenarios RCP 2.6 and RCP 8.5, may affect different aspects of



358 soil water content over the unsaturated zone for 81 large catchments worldwide. The investigated soil moisture
359 aspects include projected changes in average annual water content and in the intra-annual variability cycle around
360 this average. We have found projected changes in these aspects to be relatively small, well within modeling
361 uncertainty. Projected changes are greater for the occurrence frequency of dry and wet soil moisture events, and for
362 the average value and particularly the inter-annual variability of seasonal water content in the dry and the wet
363 seasons of the study catchments.

364 For changes in the dry/wet event occurrence (Fig. 4) and the average seasonal water content (Fig. 5), the
365 geographic patterns of change and both the magnitudes and the directions of change in individual catchments
366 depend heavily on the considered radiative forcing (RCP) scenario. The greatest changes in these event and
367 average seasonal aspects of soil moisture emerge for the RCP 8.5 scenario, with clear and physically consistent
368 large-scale geographic change patterns under the RCP 2.6 scenario shifting into spatially heterogeneous changes
369 over the world under the RCP 8.5 scenario.

370 The greatest relative changes are found for the inter-annual variability in seasonal soil water content (Fig.
371 6). The results for these changes differ from the above-described result differences between RCP scenarios in that
372 they are more or less equally large and spatially heterogeneous over the world for both RCP scenarios. However,
373 also for the inter-annual variability in seasonal water content, around half of the individual study catchments
374 exhibit opposite directions of change under the two RCP scenarios.

375 In general, the particularly large changes in inter-annual variability of seasonal soil moisture imply
376 heterogeneously changed flood and drought risks across the world. Especially the largest increases in this inter-
377 annual variability, which are found for the dry season under both RCP scenarios, indicate increased drought risks
378 for several large catchments, which need to be investigated further in focused follow-up studies.

379 **Acknowledgments**

380 This work has been supported by the Swedish University strategic environmental research program
381 Ekoklim and The Swedish Research Council Formas (project 2012-790). GPCP Precipitation data was provided by
382 the NOAA/OAR/ESRL PSD, Boulder, Colorado, USA, and is available from their Web site at
383 <http://www.esrl.noaa.gov/psd/>.



384 **References**

- 385 Asokan, S.M., Rogberg P., Bring A., Jarsjö J., Destouni G.: Climate model performance and change
386 projection for freshwater fluxes: comparison for irrigated areas in Central and South Asia, *Journal of Hydrology:*
387 *Regional Studies*, 5, 48-65, 2016.
- 388 Baldwin, M., Kellogg, C.E., Thorp, J.: Soil classification, *Soils and Men*, Yearbook of Agriculture,
389 U.S.D.A, pp. 979–1001, 1938.
- 390 Bresler, E., and Dagan, G.: Convective and pore scale dispersive solute transport in unsaturated
391 heterogeneous fields, *Water Resources Research*, 17: 1683–169, 3, 1981.
- 392 Bring, A., Asokan, S.M., Jaramillo, F., Jarsjö, J., Levi, L., Pietroń, J., Prieto, C., Rogberg, P. and
393 Destouni, G.: Implications of freshwater flux data from the CMIP5 multimodel output across a set of Northern
394 Hemisphere drainage basins, *Earth's Future*, 3(6), 206-217, doi: 10.1002/2014EF000296, 2015.
- 395 Brooks, R.H. and Corey, A.T.: Hydraulic properties of porous media, *Hydrology Papers*, Colorado State
396 University, 1964.
- 397 Corradini, C.: Soil moisture in the development of hydrological processes and its determination at
398 different spatial scales, *Journal of Hydrology*, 516, 1-5, 2014.
- 399 Dagan, G., and Bresler, E.: Solute dispersion in unsaturated heterogeneous soil at field scale: I. Theory,
400 *Soil Science Society of America Journal*, 43: 461–467, 1979.
- 401 Destouni, G.: Applicability of the steady-state flow assumption for solute advection in field soils, *Water*
402 *Resources Research*, 27: 2129–2140, 1991.
- 403 Destouni, G.: Stochastic modelling of solute flux in the unsaturated zone at the field scale, *Journal of*
404 *Hydrology*, 143: 45–61, 1993.
- 405 Destouni, G., and Cvetkovic, V.: The effect of heterogeneity on large scale solute transport in the
406 unsaturated zone, *Nordic Hydrology* 20: 43-52, 1989.
- 407 Destouni, G., and Verrot, L.: Screening long-term variability and change of soil moisture in a changing
408 climate, *Journal of Hydrology*, 516: 131–139, doi: 10.1016/j.jhydrol.2014.01.059, 2014.
- 409 Destouni G., Asokan S.M., Jarsjö J.: Inland hydro-climatic interaction: Effects of human water use on
410 regional climate, *Geophysical Res. Lett.*, 37, L18402, 2010.
- 411 Destouni G., Jaramillo F., and Prieto C.: Hydroclimatic shifts driven by human water use for food and
412 energy production, *Nature Climate Change*, 3, 213-217, 2013.



- 413 Dirmeyer, P.A., Jin, Y., Singh, B., and Yan, X.: Trends in land–atmosphere interactions from CMIP5
414 simulations, *Journal of Hydrometeorology*, 14(3), 829–849, 2013.
- 415 D’Odorico, P., Ridolfi, L., Porporato, A., and Rodriguez-Iturbe, I.: Preferential states of seasonal soil
416 moisture: The impact of climate fluctuations, *Water Resources Research*, 36(8), 2209–2219, 2000.
- 417 Entekhabi, D., Reichle, R.H., Koster, R.D., and Crow, W.T.: Performance metrics for soil moisture
418 retrievals and application requirements, *Journal of Hydrometeorology*, 11: 832–840, 2010.
- 419 FAO/IIASA/ISRIC/ISSCAS/JRC, Harmonized World Soil Database (version 1.2). FAO (Food and
420 Agriculture Organization of the United Nations), Rome, Italy and IIASA International Institute for Applied
421 Systems Analysis, Laxenburg, Austria, 2012.
- 422 GRDC, The Global Runoff Data Centre, D - 56002 Koblenz, Germany, Federal Institute of Hydrology
423 (BfG), retrieved in October 2015.
- 424 IPCC, Summary for Policymakers. In: *Climate Change 2014: Impacts, Adaptation, and Vulnerability. Part*
425 *A: Global and Sectoral Aspects. Contribution of Working Group II to the Fifth Assessment Report of the*
426 *Intergovernmental Panel on Climate Change* [Field, C.B., V.R. Barros, D.J. Dokken, K.J. Mach, M.D.
427 Mastrandrea, T.E. Bilir, M. Chatterjee, K.L. Ebi, Y.O. Estrada, R.C. Genova, B. Girma, E.S. Kissel, A.N. Levy, S.
428 MacCracken, P.R. Mastrandrea, and L.L. White (eds.)]. Cambridge University Press, Cambridge, United Kingdom
429 and New York, NY, USA, pp. 1–32, 2014.
- 430 Jaramillo F., and Destouni G.: Developing water change spectra and distinguishing change drivers
431 worldwide, *Geophysical Research Letters*, 41(23), 8377–8386, 2014.
- 432 Jaramillo, F., and Destouni, G.: Local flow regulation and irrigation raise global human water
433 consumption and footprint. *Science*, 350(6265), 1248–1251, 2015.
- 434 Jaramillo, F., Prieto C., Lyon S.W., Destouni G.: Multimethod assessment of evapotranspiration shifts due
435 to non-irrigated agricultural development in Sweden, *Journal of Hydrology*, 484, 55–62, 2013.
- 436 Jarsjö J., Asokan S.M., Prieto C., Bring A., Destouni G.: Hydrological responses to climate change
437 conditioned by historic alterations of land-use and water-use, *Hydrology and Earth System Sciences*, 16, 1335–
438 1347, 2012.
- 439 Koutsouris, A. J., Chen, D., and Lyon, S. W.: Comparing global precipitation data sets in eastern Africa: a
440 case study of Kilombero Valley, Tanzania, *International Journal of Climatology*, 2015.



- 441 Kumar, P.: A multiple scale state-space model for characterizing subgrid scale variability of near-surface
442 soil moisture, *IEEE Transactions on Geoscience and Remote Sensing*, 37: 182–197, 1999.
- 443 Kumar, S., Lawrence, D.M., Dirmeyer, P.A., and Sheffield, J.: Less reliable water availability in the 21st
444 century climate projections, *Earth's Future*, 2(3), 152–160, 2014.
- 445 Landerer, F. W., and Swenson, S. C.: Accuracy of scaled GRACE terrestrial water storage
446 estimates, *Water Resources Research*, 48(4). doi:10.1029/2011WR011453, 2012.
- 447 Mohanty, B. P., Famiglietti, J. S., and Skaggs, T. H.: Evolution of soil moisture spatial structure in a
448 mixed vegetation pixel during the Southern Great Plains 1997 (SGP97) Hydrology Experiment, *Water Resources
449 Research*, 36(12), 2000.
- 450 Morel-Seytoux, H. J., Meyer, P.D., Nachabe, M., Tourna, J., van Genuchten, M.V., and Lenhard, R.J.:
451 Parameter equivalence for the Brooks-Corey and van Genuchten soil characteristics: Preserving the effective
452 capillary drive, *Water Resources Research*, 32: 1251–1258, 1996.
- 453 Nachtergaele, F., Van Velthuisen, H., Verelst, L., Batjes, N., Dijkshoorn, K., Van Engelen, V., Fischer,
454 G., Jones A, Montanarella L, Petri M, and Prieler, S.: Harmonized world soil database, Food and Agriculture
455 Organization of the United Nations, 2008.
- 456 Oki, T., and Kanae, S.: Global hydrological cycles and world water resources. *Science*, 313(5790), 1068-
457 1072, 2006.
- 458 Peters, G. P., Andrew, R. M., Boden, T., Canadell, J. G., Ciais, P., Le Quéré, C., Marland, G., Raupach
459 M. R., and Wilson, C.: The challenge to keep global warming below 2 C, *Nature Climate Change*, 3(1), 4-6, 2013.
- 460 Rawls, W.J., Brakensiek, D.L. and Saxton, K.E.: Estimation of soil water properties, *Transactions of the
461 American Society of Agricultural Engineers*, 25: 1316–1320, 1982.
- 462 Riahi, K., Rao, S., Krey, V., Cho, C., Chirkov, V., Fischer, G., Kindermann, G., Nakicenovic, N. and
463 Rafaj, P.: RCP 8.5—A scenario of comparatively high greenhouse gas emissions, *Climatic Change*, 109(1-2), 33-
464 57, 2011.
- 465 Russo, D.: Stochastic analysis of flow and transport in unsaturated heterogeneous porous formation:
466 Effects of variability in water saturation, *Water Resources Research*, 34: 569–581, 1998.
- 467 Saxton, K.E., Rawls, W., Romberger, J.S. and Papendick, R.I.: Estimating generalized soil-water
468 characteristics from texture, *Soil Science Society of America Journal*, 50: 1031–1036, 1986.



- 469 Schneider, U., Becker, A., Finger, P., Meyer-Christoffer, A., Rudolf, B., and Ziese, M.: GPCP full data
470 reanalysis version 6.0 at 0.5°: monthly land-surface precipitation from rain-gauges built on GTS-based and historic
471 data. doi: 10.5676/DWD_GPCC_FD_M_V6_050, 2011.
- 472 Seneviratne, S.I., Corti, T., Davin, E.L., Hirschi, M., Jaeger, E.B., Lehner, I., Orlowsky, B. and Teuling
473 A.J.: Investigating soil moisture–climate interactions in a changing climate: A review, *Earth-Science Reviews*, 99:
474 125–161, 2010.
- 475 Sillmann, J., Kharin, V.V., Zhang, X., Zwiers, F. W., and Bronaugh, D.: Climate extremes indices in the
476 CMIP5 multimodel ensemble: Part 1. Model evaluation in the present climate. *Journal of Geophysical Research:*
477 *Atmospheres*, 118(4), 1716-1733, 2013.
- 478 Swenson, S.C.: GRACE monthly land water mass grids NETCDF RELEASE 5.0. Ver. 5.0. PO.DAAC,
479 CA, USA. Dataset accessed 2015-12-02 at <http://dx.doi.org/10.5067/TELND-NC005>, 2012.
- 480 Swenson, S., and Wahr, J.: Post-processing removal of correlated errors in GRACE data, *Geophysical*
481 *Research Letters*, 33(8), doi:10.1029/2005GL025285, 2006.
- 482 Taylor, K.E., Stouffer, R. J., and Meehl, G.A.: An overview of CMIP5 and the experiment
483 design, *Bulletin of the American Meteorological Society*, 93(4), 485-498. doi:10.1175/BAMS-D-11-00094.1,
484 2012.
- 485 Törnqvist, R., Jarsjö, J., Pietrón, J., Bring, A., Rogberg P., Asokan S.M., Destouni G.: Evolution of the
486 hydro-climate system in the Lake Baikal basin, *Journal of Hydrology*, 519, 1953–1962, 2014.
- 487 USGS, U.S. Geological Survey, Department of the Interior/USGS, Groundwater level data retrieved from
488 <http://waterdata.usgs.gov/nwis/gw> in February 2015.
- 489 van Genuchten, M.T.: A closed-form equation for predicting the hydraulic conductivity of unsaturated
490 soils, *Soil Science Society of America Journal*, 44: 892–898, 1980.
- 491 van Vuuren, D.P., Den Elzen, M.G., Lucas, P.L., Eickhout, B., Strengers, B. J., van Ruijven, B., Wonink,
492 S. and van Houdt, R.: Stabilizing greenhouse gas concentrations at low levels: an assessment of reduction
493 strategies and costs, *Climatic Change*, 81(2), 119-159 doi:10.1007/s10584-006-9172-9, 2007.
- 494 Verrot, L., and Destouni, G.: Screening variability and change of soil moisture under wide-ranging
495 climate conditions: Snow dynamics effects, *Ambio*, 44(1), 6-16, doi: 10.1007/s13280-014-0583-y, 2015.
- 496 Verrot, L., and Destouni, G.: Data-model comparison of variability in long-term time series of large-scale
497 soil moisture, In review, 2016.



498 WMO, Composition of the WMO, World Meteorological Organization, WMO-OMM-No5, CH-1211
499 Geneva 2, Switzerland, 2014.

500 Wu, W.Y., Lan, C.W., Lo, M.H., Reager, J.T., and Famiglietti, J.S.: Increases in the Annual Range of Soil
501 Water Storage at Northern Mid- and High-Latitudes under Global Warming, Geophysical Research Letters, 42(10),
502 3903-3910, 2015.

503 Figure captions

504 **Figure 1: Map of the location of the 81 study catchments. The used region acronyms in the**
505 **catchment numbering cluster the catchments according to the WMO region classification (WMO, 2014):**
506 **“Nam” stands for North-America, “Sam” for South-America, “Eur” for Europe, “Swp” for South-west**
507 **Pacific, “Afr” for Africa and “Asi” for Asia.**

508

509 **Figure 2: (a) Map of a set of hydrological catchments in the tropics, for which Verrot and Destouni**
510 **(2016) have compared the unsaturated water content model expressed by the second part of main Eq. (1)**
511 **with GRACE satellites data for large-scale water storage change. The model-data comparison results are**
512 **here exemplified for two of the catchments: (b) Afr4 and (c) Sam11. Results in panels (b,c) show the**
513 **comparison of model results (pink thinner line) with the GRACE-derived data (purple thicker line) for**
514 **large-scale water storage change. The model results are based on unsaturated water content quantification**
515 **through the second part of Eq. (1), by compiling CSR-RL05 GRACE data from Swenson (2012), Landerer and**
516 **Swenson (2012), and Swenson and Wahr (2006) for direct comparison with corresponding model output, and**
517 **synthesizing as model inputs for each catchment available independent runoff data for the same time period**
518 **from (GRDC, 2015) with calibrated γ factor for effective runoff R_{eff} , along with independent soil-characteristic**
519 **data from the Harmonized World Soil Database v1.1 (Nachtergaele et al., 2008; FAO, 2012), and in addition**
520 **also evaluating a complementary water storage change component of groundwater level change using**
521 **fundamental catchment-scale flux water balance based equation (2) in Verrot and Destouni (2015) and**
522 **associated required additional inputs of independent data for precipitation and evapotranspiration from the**
523 **Global Precipitation Climatology Center (GPCC, Schneider et al., 2011) and MODIS product (ORNL DAAC,**
524 **2011).**

525



526 **Figure 3: Mean monthly relative degree of water saturation over the unsaturated soil zone. Results**
527 **are shown for 6 study catchment examples (1 from each WMO region, Fig. 1), for two radiative forcing**
528 **(RCP) scenarios (red and pink lines for RCP 2.6, blue and green lines for RCP 8.5), and for the two study**
529 **periods (red and blue lines for 2006-2025, pink and green lines for 2080-2099). The solid lines represent the**
530 **ensemble mean model result and the dashed lines represent 1 standard deviation around the mean of the**
531 **corresponding result derived from individual models. The relative degree of soil water saturation (with**
532 **value 1 corresponding to full saturation) represents the unsaturated soil water content normalized by the**
533 **saturated soil water content (soil porosity). The month numbering is: January as month 1 through to**
534 **December as month 12.**

535

536 **Figure 4: Map of relative change from 2006-2025 to 2080-2099 in the frequency of relatively dry**
537 **(two upper panels a and b) and wet (two lower panels c and g) soil moisture events. Results are shown for**
538 **the radiative forcing scenarios RCP 2.6 (panels a and c) and RCP 8.5 (panels b and d) in terms of relative**
539 **change (%) from the original frequency of 5% for both types of events (dry water content below the 5**
540 **percentile value and wet water content above the 95 percentile value) in 2006-2025 to the resulting**
541 **frequency of these water content values in 2080-2099.**

542

543 **Figure 5: Map of relative change in mean seasonal water content over the unsaturated zone. Results**
544 **are shown for the dry season (two upper panels a and b) and the wet season (two lower panels c and g), and**
545 **the two radiative forcing scenarios RCP 2.6 (panels a and c) and RCP 8.5 (panels b and d) in terms of**
546 **relative change (in %) from 2006-2025 to 2080-2099.**

547

548 **Figure 6: Map of relative change in the inter-annual variability of seasonal water content over the**
549 **unsaturated zone. Results are shown for the dry season (upper panels a and b) and the wet season (lower**
550 **panels c and g) and the two radiative forcing scenarios RCP 2.6 (panels a and c) and RCP 8.5 (panels b and**
551 **d) in term of relative change (in %) from 2006-2025 to 2080-2099.**

552



Figure 1

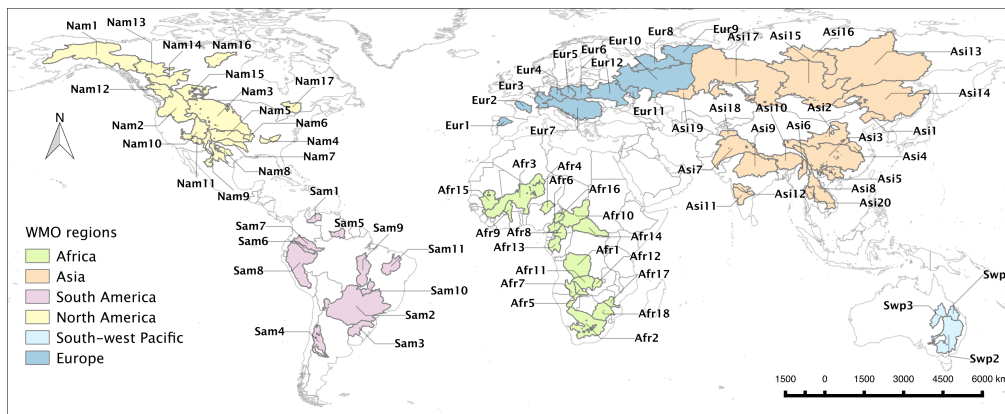
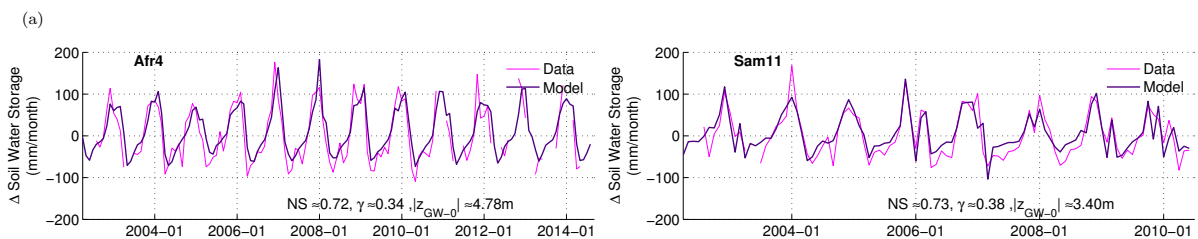
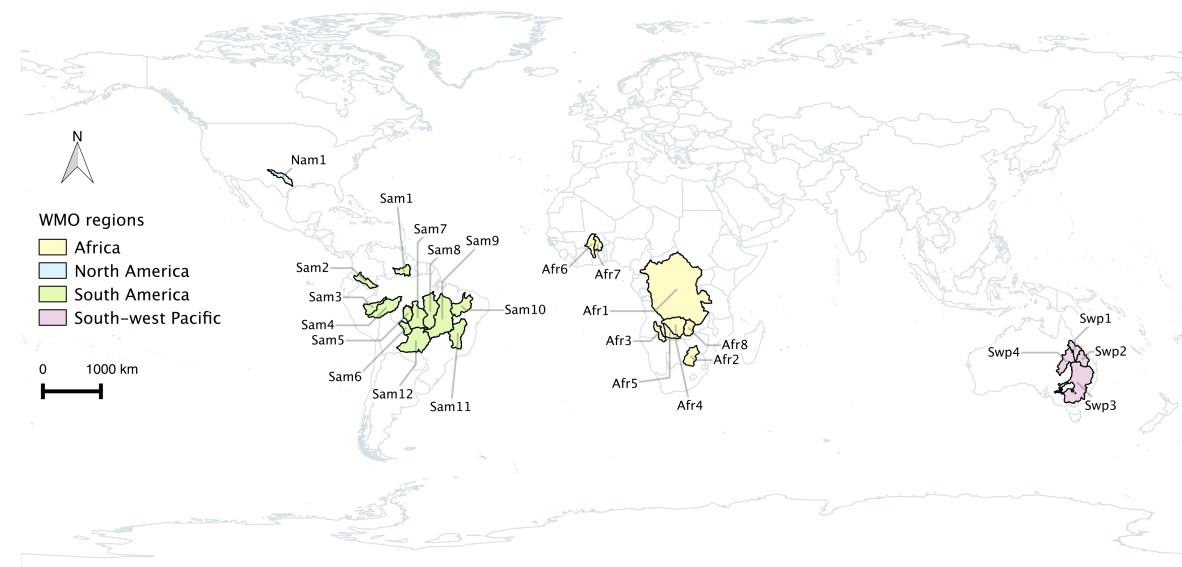




Figure 2



(b)

(c)



Figure 3

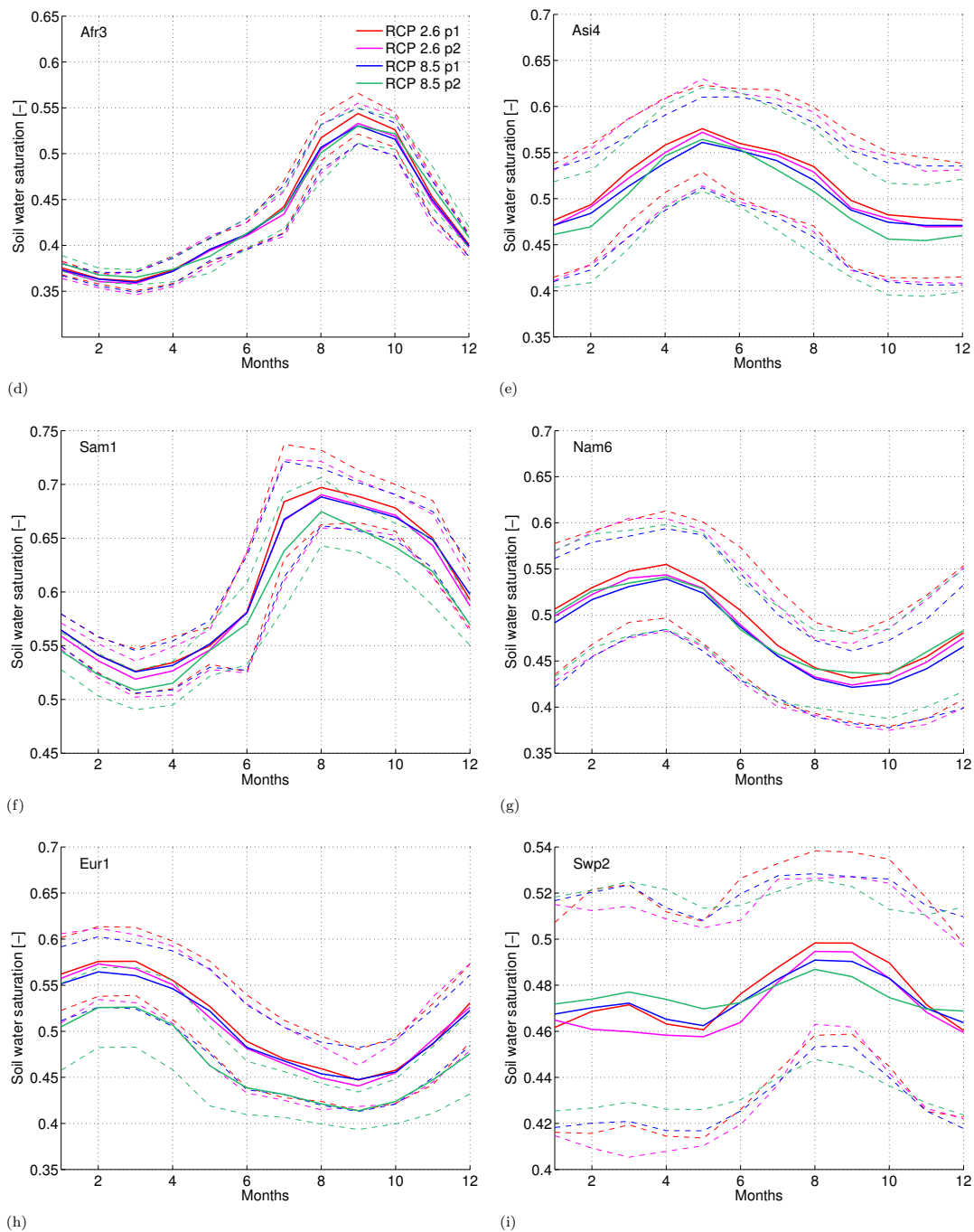




Figure 4

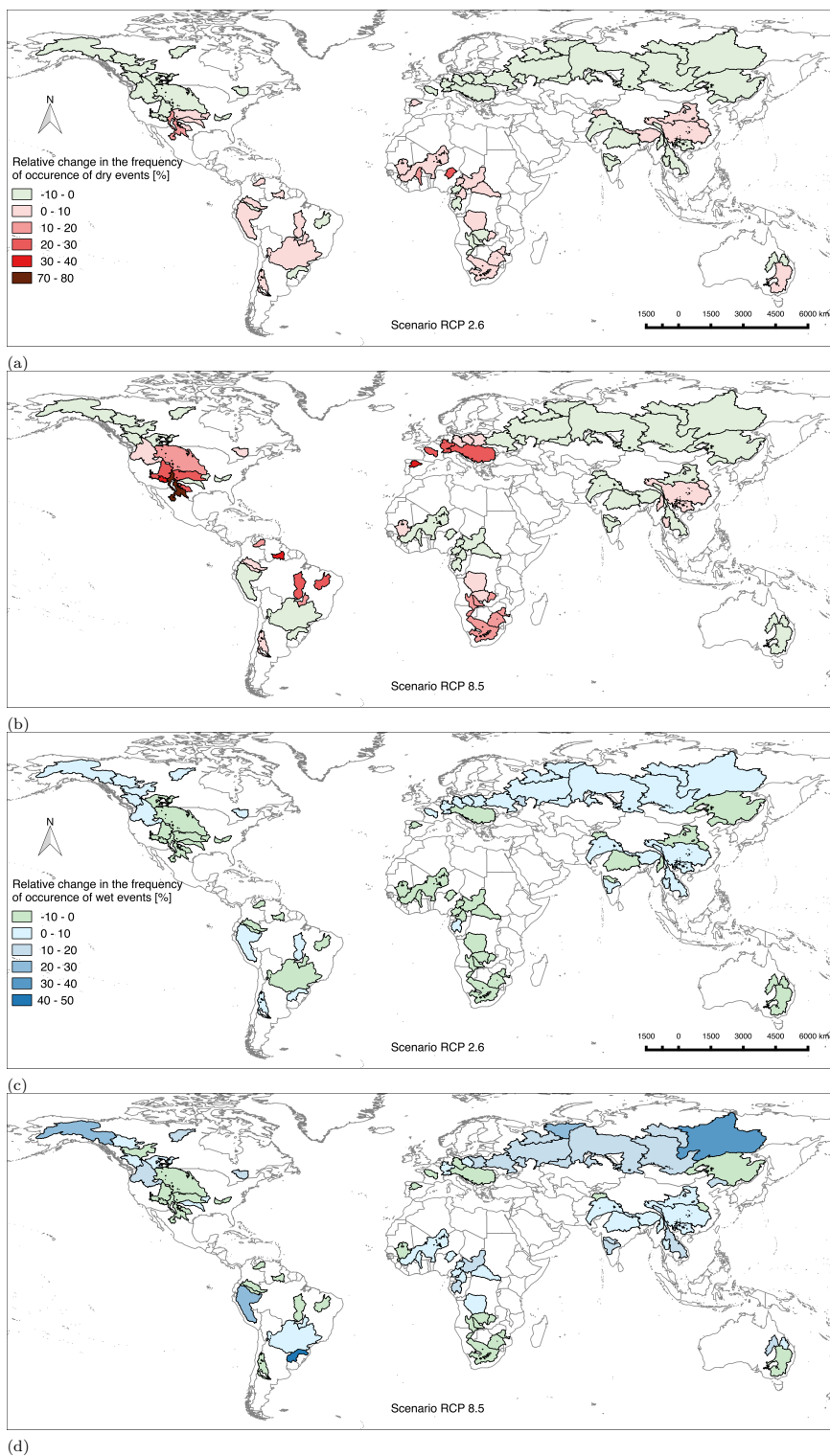




Figure 5

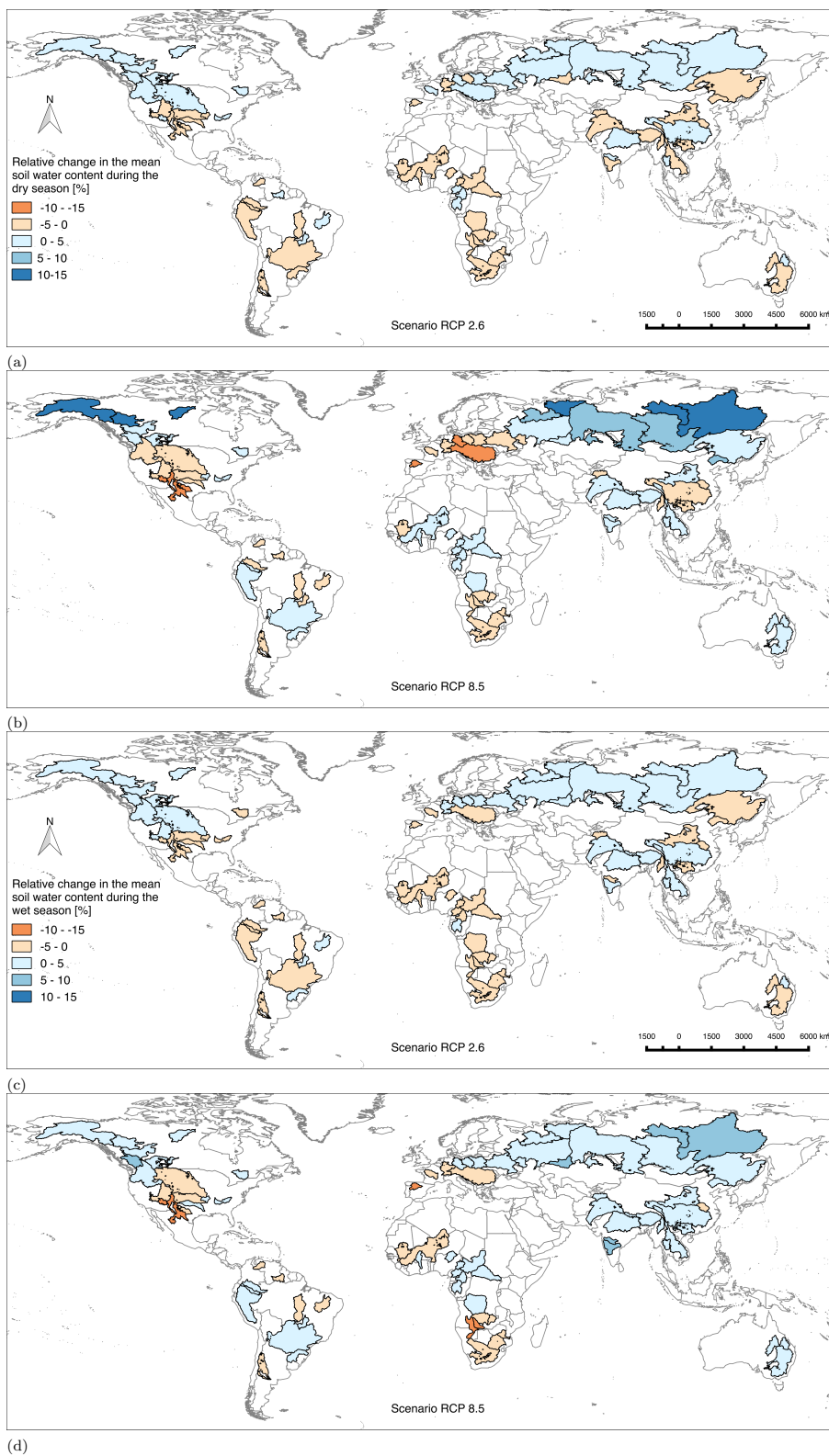




Figure 6

